2D attenuated total reflectance infrared spectroscopy reveals ultrafast vibrational dynamics of organic monolayers at metal-liquid interfaces

Kraack, Jan Philip ; Lotti, Davide ; Hamm, Peter

Abstract: We present two-dimensional infrared (2D IR) spectra of organic monolayers immobilized on thin metallic films at the solid liquid interface. The experiments are acquired under Attenuated Total Reflectance (ATR) conditions which allow a surface-sensitive measurement of spectral diffusion, sample inhomogeneity, and vibrational relaxation of the monolayers. Terminal azide functional groups are used as local probes of the environment and structural dynamics of the samples. Specifically, we investigate the influence of different alkyl chain-lengths on the ultrafast dynamics of the monolayer, revealing a smaller initial inhomogeneity and faster spectral diffusion with increasing chain-length. Furthermore, by varying the environment (i.e., in different solvents or as bare sample), we conclude that the most significant contribution to spectral diffusion stems from intra-and intermolecular dynamics within the monolayer. The obtained results demonstrate that 2D ATR IR spectroscopy is a versatile tool for measuring interfacial dynamics of adsorbed molecules.

DOI: https://doi.org/10.1063/1.4916915

AIP | The Journal of Chemical Physics

2D attenuated total reflectance infrared spectroscopy reveals ultrafast vibrational dynamics of organic monolayers at metal-liquid interfaces

Jan Philip Kraack, Davide Lotti, and Peter Hamm

Citation: The Journal of Chemical Physics **142**, 212413 (2015); doi: 10.1063/1.4916915
View online: http://dx.doi.org/10.1063/1.4916915
View Table of Contents: http://scitation.aip.org/content/aip/journal/jcp/142/21?ver=pdfcov
Published by the AIP Publishing

2D attenuated total reflectance infrared spectroscopy reveals ultrafast vibrational dynamics of organic monolayers at metal-liquid interfaces

Jan Philip Kraack, Davide Lotti, and Peter Hamm[a)]
Department of Chemistry, University of Zurich, Winterthurerstrasse 190, 8057 Zurich, Switzerland

(Received 9 December 2014; accepted 23 March 2015; published online 6 April 2015)

We present two-dimensional infrared (2D IR) spectra of organic monolayers immobilized on thin metallic films at the solid liquid interface. The experiments are acquired under Attenuated Total Reflectance (ATR) conditions which allow a surface-sensitive measurement of spectral diffusion, sample inhomogeneity, and vibrational relaxation of the monolayers. Terminal azide functional groups are used as local probes of the environment and structural dynamics of the samples. Specifically, we investigate the influence of different alkyl chain-lengths on the ultrafast dynamics of the monolayer, revealing a smaller initial inhomogeneity and faster spectral diffusion with increasing chain-length. Furthermore, by varying the environment (i.e., in different solvents or as bare sample), we conclude that the most significant contribution to spectral diffusion stems from intra- and intermolecular dynamics within the monolayer. The obtained results demonstrate that 2D ATR IR spectroscopy is a versatile tool for measuring interfacial dynamics of adsorbed molecules. © *2015 AIP Publishing LLC*. [http://dx.doi.org/10.1063/1.4916915]

INTRODUCTION

Molecular properties at solid-liquid interfaces are of particular importance in chemistry and physics, for instance, concerning heterogeneous reaction dynamics or electrochemistry.[1–7] This holds for solvent molecules in the direct vicinity of the solid-liquid interface as well as for molecules which are chemically or physically adsorbed on the solid side. It is highly desirable to gain spectroscopic insight into interfacial systems such as heterogeneous catalytically active surfaces,[2,3,5] dye-sensitized solar cells,[8,9] or self-assembled monolayers[10,11] (MLs). Particularly, MLs of organic molecules and metal-complexes play a key role in several branches of industrial and scientific research. Such systems find a broad range of applications, for instance, in organic electronics,[12] molecular sensing,[13] or in biophysics[14] and medicinal applications.[15] Their usefulness as well as their relatively simple preparation has promoted organic MLs to central building blocks in interfacial science and technology.

Regarding spectroscopic investigations of MLs at interfaces, central points of interest are represented by details of binding configurations or influences of the environmental interactions on molecular properties as compared to the case of isolated molecules in bulk solution.[16–19] This is because the structure of molecules in MLs is often influenced by intermolecular interactions within the densely packed aggregate.[20,21] In addition, solvent molecules directly at the interface are likely to exhibit differences in their properties such as hydrogen-bonding networks and dipolar orientation as compared to the bulk solvent.[4,22,23] In this context, ultrafast infrared (IR) spectroscopy in its various forms has been proven to be a useful tool to unravel changes in molecular structure and dynamics, which occur down to the femtosecond time scale.[16–19] In particular, multi-dimensional techniques[17,24–27] have been developed in recent years as powerful methods to tackle the issues mentioned above. These techniques are sensitive to, e.g., structural heterogeneity and flexibility, energy transfer, or intermolecular interactions, signatures of which are challenging to extract unambiguously from conventional (1D) vibrational spectra.[28,29]

We recently developed a new method to acquire two-dimensional (2D) IR spectra from molecules at interfaces by means of ultrafast attenuated total reflectance (ATR) IR spectroscopy.[25] The 2D ATR IR method is a straight-forward to implement technique, which exploits the evanescent electric field that occurs under total reflectance conditions[30,31] if light impinges on an interface that is composed of materials with different refractive indices ($n_{1/2}$, Fig. 1). The evanescent field can excite and subsequently interrogate molecular dynamics within the penetration depth of the light into the material of lower refractive index ($n_2 < n_1$). The penetration depth is on the order of the optical wavelength of the employed light wave.[2] The experiment is analogous to ordinary 2D spectroscopy in pump-probe[32,33] geometry. The overall 2D ATR IR signal therefore depends on the third-order nonlinear susceptibility and can be directly compared to results from, e.g., transmission 2D IR spectroscopy. In this sense, 2D ATR IR spectroscopy can be regarded as a surface-sensitive technique since the maximum intensity for excitation and probing is available directly at the interface. The method is, however, not surface-specific since all molecules within the penetration depth can absorb energy from the evanescent field and therefore can contribute to the nonlinear signal. This makes the 2D ATR IR technique different from alternative methods such as ultrafast 2D vibrational sum-frequency generation (SFG)[26,27,34] spectroscopy which is truly surface-specific, since in this case,

[a)]Author to whom correspondence should be addressed. Electronic mail: peter.hamm@chem.uzh.ch; Telephone: +41 44 63 544 31; Fax: +41 44 63 568 38.

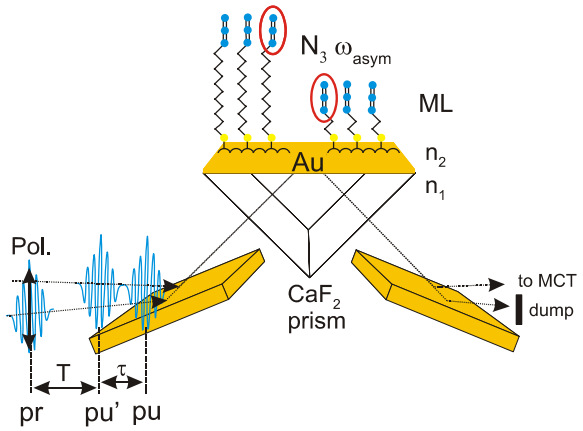

FIG. 1. Experimental configuration of 2D ATR IR spectroscopy in pump-probe geometry. Two collinear, coherent, femtosecond pump (pu/pu′) and a probe pulse (pr) excite and interrogate the dynamics of organic MLs by evanescent fields within the penetration depth in the medium of lower refractive index ($n_2 < n_1$). The MLs are equipped with a local vibrational probe, i.e., the asymmetric stretch vibration of the azide group (N_3). The polarization is indicated for the probe pulse.

the even order nonlinear process requires a breakdown of inversion-symmetry, which occurs at the interface.

In this paper, we present 2D ATR IR spectroscopy of the ultrafast dynamics of organic MLs on thin metallic surfaces. We investigate the dynamics of MLs from linear alkyl-thiols of different chain lengths, which are attached to a gold-coated ATR prism. Within the MLs, we use the asymmetric stretch vibration of a terminal azide functional group as a local probe of the interactions of the MLs to their environment (Fig. 1). We find that immobilization of the molecules in the MLs decelerates spectral diffusion dynamics of the azide group, as compared to typical values in bulk solution. In addition, an increase in chain length between the azide probe and the metal surface results in a reduced correlation between pump- and probe frequencies in the MLs for all investigated waiting times. Moreover, environmental influences on the vibrational dynamics are investigated by measurements of bare MLs versus MLs immersed in solvent of different polarities as well as hydrogen-bonding capabilities and different properties of the metal layers. It is found that the dominant contribution to spectral diffusion within the MLs stems from intra- and intermolecular conformational dynamics. Finally, it is shown by an isotope dilution experiment that no couplings among the azide groups of the ML molecules exist. The presented results show that 2D ATR IR spectroscopy is a powerful method to investigate the ultrafast vibrational dynamics of molecules at interfaces.

MATERIALS AND METHODS

Laser setup

The concept of the ultrafast 2D ATR IR experiment has been introduced previously.[25] In brief, a chirped-pulse amplifier system (Spectra Physics, Spitfire), which delivers ≈90 fs pulses centered at 800 nm, is operated at 5 kHz to pump a two-stage optical parametric amplifier (OPA).[35] The OPA delivers ≈90–100 fs pulses with a bandwidth (full-width at half maximum (FWHM)) of ≈250 cm^{-1} and a total of ≈1.3 μJ per pulse at typical central frequencies around 2100 cm^{-1}. The OPA output is split into pump (≈90%) and probe/reference beams (each ≈5%) with a BaF_2 wedge, the former of which is used to generate coherent, collinear pump pulse pairs in a Mach-Zehnder interferometer for two-dimensional spectroscopy in pump-probe configuration.[32] The final maximum pump pulse energy exiting the interferometer is ≈800 nJ per pulse. Pump and probe/reference beams are focused in a home-built, single reflection ATR sample cell onto the backside of a commercial CaF_2 prism (10 × 10 mm, Thorlabs). CaF_2 is used as an ATR crystal, since the more common materials, such as ZnSe or Si, show a nonlinear response due to multi-photon absorption of the intense IR pulses. The entrance angle of all three beams with respect to the normal of the reflecting plane of the CaF_2 prism is large (85°) due to the small index of refraction of CaF_2. Pump, probe, and reference beams (the latter not shown in Fig. 1) have mutual angles of ≈5°–7°. All three beams lie in a common plane and exhibit p-polarization with respect to the reflecting CaF_2 surface. Probe and reference beams are detected by a 2 × 32 pixel MCT array detector (Infrared Associates) equipped with a grating spectrograph (Jobin-Yvon Triax, 150 lines/mm) to give a balanced signal.

Sample preparation

CaF_2 prisms were sputter-coated with gold (Au) in a Baltec SCD 500 sputter coater at the Center for Microscopy and Image Analysis (University of Zürich). Prior to sputtering, the prisms were carefully cleaned with ethanol and doubly deionized water. Typically, the base pressure for the sputtering process was set to 8×10^{-5} millibars of argon, and the sputter process was conducted at 0.1 millibars. The average thickness of the metal layers on the prisms was determined with a quartz-microbalance. The applied current for the sputtering process was generally 6–8 mA, which resulted in a sputtering rate of 0.02 nm s^{-1} at a working distance of 50 mm.

2-azidoethanthiol (2-N3) and 11-azidoundecanethiol (11-N3) samples (Figure 1) were synthesized following standard procedures using commercially available starting materials (reagent grade, Sigma-Aldrich).[36,37] For the isotope substituted sample, the same procedure could be used, using triply isotope-labeled $Na^{15}N_3^-$ as starting material instead. For the formation of the MLs, sample solutions in spectroscopic grade ethanol (Sigma Aldrich or Carl Roth) were diluted to a concentration of 1 mM. Au-coated CaF_2 prisms were incubated in independent, tightly closed beakers of thoroughly cleaned glassware for 10 h. The kinetics of the ML formation were independently monitored by the use of temporal evolution of the IR absorption at ≈2100 cm^{-1} in a Fourier transform (FT)-IR spectrometer. Adsorption was complete after ≈10–12 h of incubation. Formation of MLs on Au surfaces was verified on independent samples by UV-light induced desorption experiments (wavelength 370 nm), which break the Au–S bond. Following the incubation, the Au-coated prisms were thoroughly washed with ethanol and subsequently with doubly deionized water followed by a drying procedure in a stream on nitrogen. The freshly prepared ML samples generated in this way were stable both in air as well as immersed in several solvents (diethylether (DEE), acetonitrile (MeCN), or methanol (MeOH)), and sta-

tionary absorption characteristics were found to be unaltered by flowing extensive amounts of solvent above the ML coated prism in a home-built sample flow cell. The ultrafast experiments also did not result in any change of the stationary absorption spectra of the samples.

RESULTS

From absorption measurements in transmission of 11-N3 and 2-N3 in bulk solution, we know that the extinction coefficient of the asymmetric stretch vibration of the azide group is 550–600 M^{-1} cm^{-1}; that is, it is only a medium-strong infrared absorber. Fig. 2 shows linear ATR spectra of 2-N3 and 11-N3 as MLs on 1 nm Au coated CaF_2 prisms incubated in various solvents (MeCN, MeOH, and DEE) as well as bare ML without any solvent, *in-situ* measured in the ultrafast 2D spectrometer by the MCT detector. In the bare ML case, the MLs were carefully dried from solvent and kept in a continuous stream of nitrogen during the measurements. The spectra have been obtained by consecutive acquisition of background spectra and sample spectra from reflections of the ATR crystal. For the background spectra, independently co-sputtered CaF_2 prisms have been used and incubated with the same solvent. Calculation of $-\log(I_{smp}/I_{ref})$ yields the corresponding absorption spectrum. It is guaranteed by the preparation method of the MLs as well as from the performed control experiments (see section on Materials and Methods) that the absorption exclusively stems from immobilized molecules on the surface and not from any contributions from the bulk solution.

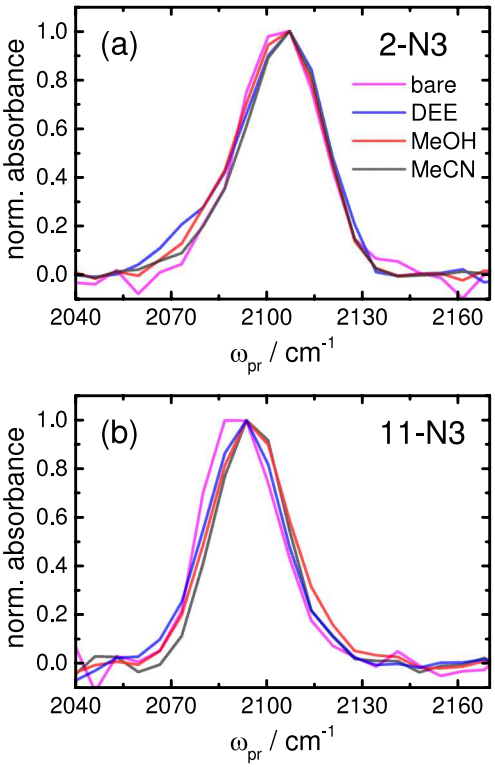

FIG. 2. Normalized linear absorption spectra of (a) 2-azidoethanthiol (2-N3) and (b) 11-azidoundecanethiol (11-N3) MLs on 1 nm Au coated CaF_2 prisms incubated with different solvents (MeCN in black, MeOH in red, and DEE as blue), and as bare ML (magenta). Exemplified for MeCN, peak absorption values are 25 mOD (2-N3) and 18 mOD (11-N3).

Fig. 2 shows that the spectra hardly depend on the environment, i.e., whether they are incubated in a solvent or on the nature of the solvent, indicating a rather low degree of interaction between solvent molecules and the azide vibrational probe. Taking MeCN as an example, the spectra exhibit a single band at ≈2105 cm^{-1} (2-N3) or 2095 cm^{-1} (11-N3), which is due to the asymmetric stretch vibration of the azide functional group attached at the end of the alkyl chains. Values of FWHM are determined to ≈32 cm^{-1} (2-N3) and 30 cm^{-1} (11-N3), respectively, in agreement with typical spectra of similar molecules containing azide groups attached to alkyl chains in organic molecules both in bulk solution[38–40] and immobilized on a surface.[36,37,41] Also in terms of the peak size, the data presented here agree with previously reported values for different ML sample systems.[36,42–44] Note that the peak absorbance of ML samples at metal surfaces is likely to be influenced by local field surface-enhancement effects,[42,45–47] which will contribute to the 2D ATR IR spectroscopy as well, an effect that is currently under investigation and will be published as a separate account.

Absorptive 2D ATR IR spectra of solvent-incubated 2-N3 MLs adsorbed on a 1 nm Au film are presented in Figs. 3(a) and 3(b), whereas Figs. 3(c) and 3(d) show bare MLs. The combined ground-state bleach/stimulated emission (GSB/SE) signals are depicted in blue and excited state absorption (ESA) signals are depicted in red. The signal amplitudes decay due to vibrational relaxation with time constants of 1.5 ± 0.3 ps and 1.7 ± 0.2 ps for the solvent-immersed and bare MLs, respectively, which limits the maximum observation window to 10 ps (the data are normalized in Fig. 3). At early population times (0.15 ps), the GSB/SE and ESA signals are strongly elongated along the diagonal line, indicating an inhomogeneous broadening of the absorption band. Later stages of relaxation

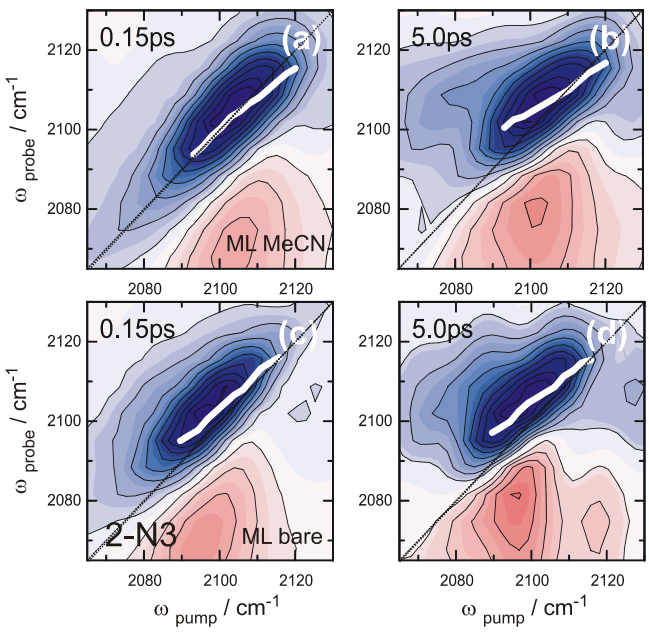

FIG. 3. Absorptive 2D IR spectra of MLs of 2-azidoethanthiol (2-N3) on a 1 nm Au layer immersed in MeCN (panels (a) and (b)), and as a bare ML (panels (c) and (d)) at representative population times (0.15 ps and 5 ps). Signal intensities have been normalized to the GSB/SE signals in order to facilitate comparison.

(5 ps) exhibit similar GSB/SE and ESA features, again strongly elongated along the diagonal. This is independent of immersion of the ML with a solvent.

The center line slope (CLS) of, e.g., the GSB/SE signal (represented as a white line in Fig. 3) can be used to quantify the amount of diagonal elongation of the peak.[48] Similar values for the CLS are observed at 0.15 ps (slopes of ≈0.8, Figs. 3(a) and 3(c)) for both the solvent-incubated and bare MLs, whereas slight differences exist at a later stage at 5 ps (≈0.62, Fig. 3(b) versus ≈0.7, Fig. 3(d)). However, only a minor temporal evolution of the CLSs occurs in both cases.

In order to elucidate the impact of varying distances between the azide probe and the Au surface, Fig. 4 shows the same set of experiments for 11-N3 with a longer alkyl chain under otherwise identical conditions. Vibrational relaxation is faster for 11-N3 (0.9 ± 0.1 ps and 1.1 ± 0.1 ps for solvent-incubated MLs and bare MLs, respectively), limiting the maximum observation window to 5 ps in this case. With respect to the diagonal elongation of the signals, the trend is the same as for 2-N3, but with overall speaking significantly smaller CLSs.

A detailed analysis of the evolution of the CLSs as a function of population times is shown in Fig. 5, which reveals the underlying dynamics of spectral diffusion.[48] Taking MLs of 2-N3 in MeCN as an example (black circles, Fig. 5), the CLSs start at values of ≈0.8 and evolve to a value of about 0.55 within 10 ps. The observed temporal evolution suggests an exponential decay of the CLS, but we cannot observe full convergence of the CLS' decay due to the limited observation window. We fitted the experimental data with a model consisting of a single exponential function and a constant offset ($CLS(T) = \Delta_1 \exp(-T/\tau_{SD}) + \Delta_2$). However, due to the limited time window, we cannot decide whether the offset Δ_2 is truly

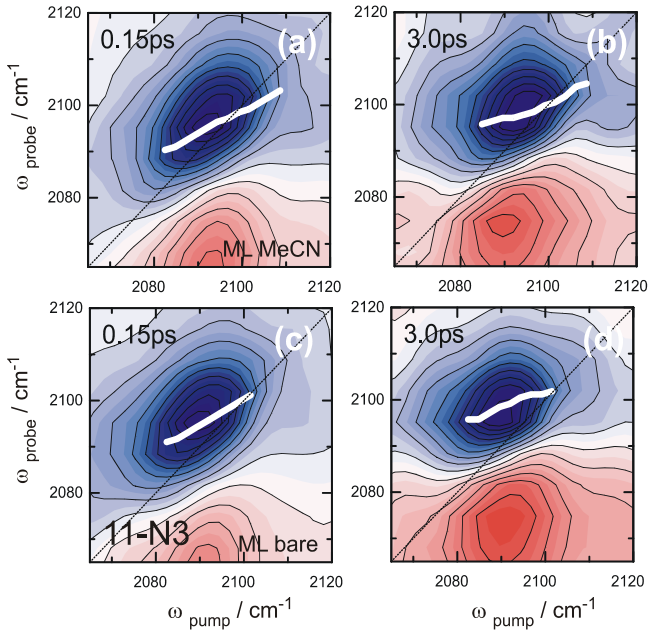

FIG. 4. Absorptive 2D IR spectra of MLs of 11-azidoundecanthiol (11-N3) on a 1 nm Au layer immersed in MeCN (panels (a) and (b)), and as a bare ML (panels (c) and (d)) at representative population times (0.15 ps and 3 ps). Signal intensities have been normalized to the GSB/SE signals in order to facilitate comparison.

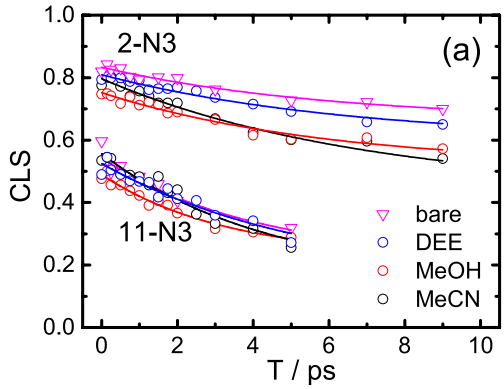

FIG. 5. CLS dynamics of 2-N3 and 11-N3 MLs on a 1 nm Au layer incubated in MeCN (black), MeOH (red), and DEE (blue), as well as bare ML (magenta). Open symbols represent experimental data while solid lines represent exponential fits as described in the text. The fit parameters are summarized in Table I (2-N3) and Table II (11-N3).

static due to a heterogeneity of the surface, for example, or whether it is related to additional dynamic processes on time scales slower than our observation window. Furthermore, one needs to keep in mind that the errors in the fit parameters are strongly correlated. For 2-N3 in MeCN, the best fit reveals a time constant of 7 ± 2 ps together with an offset of $\Delta_2 \approx 0.44$, but if one were to force the fit to decay to zero (i.e., $\Delta_2 = 0$), the time constant would be lengthened to $\tau_{SD} \approx 25$ ps with only modestly increased root-mean-square-deviation (rmsd) of the fit (+20%).

Similar dynamics for spectral diffusion of the 2-N3 MLs are observed in different solvation environments (Fig. 5). For the total set of solvents, acetonitrile (MeCN) and methanol (MeOH) have been chosen because of their similar polarity but different hydrogen-bonding capability. In addition, ML immersed in DEE as an apolar, non-hydrogen-bonding solvent as well as bare MLs (magenta) has been investigated. In case of the 2-N3 MLs, all curves start at a CLS of ≈0.8 but decay to slightly different values within ≈10 ps, i.e., somewhat lower for stronger interacting solvent environments (MeCN and MeOH *versus* DDE and bare). That is, Δ_2 values (offsets) increase with lower polarity of the environment while Δ_1 (dynamic amplitude) values decrease by about the same amount (Table I). The time constants (τ_{SD}) extracted from the fits are all about the same within the experimental uncertainty (6-8 ps, Table I).

Also in case of the 11-N3 MLs, all curves are very similar to each other. The initial values of the CLSs (between 0.5 and 0.6) are lower than for 2-N3, irrespective of the chemical environment. The decay time constants (τ_{SD}) are faster than for 2-N3 MLs and show no clear differences for the chosen solvents (Table II). In addition, also the offsets from the fits

TABLE I. Fit parameters deduced from the CLSs of 2-N3 MLs immersed in different solvents.

ML	T_1/ps	τ_{SD}/ps	Δ_1	Δ_2
MeCN	1.5 ± 0.3	7.0 ± 2.1	0.35	0.44
MeOH	1.4 ± 0.2	6.0 ± 1.7	0.24	0.52
DEE	1.5 ± 0.1	7.6 ± 1.6	0.21	0.60
Bare	1.7 ± 0.2	6.1 ± 2.1	0.17	0.67

TABLE II. Fit parameters deduced from the CLSs of 11-N3 MLs immersed in different solvents.

ML	T_1/ps	τ_{SD}/ps	Δ_1	Δ_2
MeCN	0.9 ± 0.1	4.4 ± 0.4	0.41	0.15
MeOH	0.9 ± 0.1	3.4 ± 0.5	0.28	0.21
DEE	0.9 ± 0.2	5.5 ± 0.5	0.37	0.15
Bare	1.1 ± 0.1	4.0 ± 1.3	0.34	0.22

are all in the same range ($\Delta_2 \approx 0.15$–0.22). Thus, the spectral diffusion dynamics are largely independent of the environment (even in the absence of a solvent).

In order to elucidate influences of the Au layers on the dynamics of the MLs, spectral diffusion was monitored in dependence of the average sputtered thickness of the supporting metal layer as well. Figure 6 shows CLS curves for 2-N3 immobilized on Au surfaces of different average thicknesses ranging from 0.1 nm to 1.5 nm. The surfaces were prepared by otherwise analogous preparation procedures, and the ML samples were all incubated with MeCN as a solvent. All curves start at ≈0.8 and decay to values around 0.6 within 10 ps. Application of exponential fits to the data reveals time constants between 5.5 ± 1.0 ps (0.1 nm) and 7.4 ± 2.8 ps (1.5 nm) together with offsets which range between 0.45 and 0.55. Taking into account the corresponding confidence intervals for the fits, these values can be considered as similar. It is therefore concluded that spectral diffusion is influenced by the thickness of the metal layer only to a minor extent.

A possible source of spectral diffusion is Förster-like vibrational energy transfer between different molecules.[16,49–53] In this case, one molecule is initially excited but subsequently transfers its excitation energy to another oscillator that may have a different transition frequency. Such a mechanism may be particularly relevant in ML samples, where the vibrational probes are fairly close to each other. The cleanest test whether such a mechanism contributes to spectral diffusion is an isotope dilution experiment.[51–53] This is reasoned by the fact that the Förster-type mechanism is a resonant effect with a strong (r^{-6}) distance dependence. Hence, upon isotope dilution, the spectral diffusion rate should decrease significantly as the absorption frequencies are shifted out of resonance. At the same time, isotope dilution does not at all affect the local structure of the ML sample.

We recorded 2D ATR IR data of mixed monolayers (MMLs) containing all ^{14}N azide groups (11-N3) as well as fully isotope-labelled all ^{15}N azide probes (11-N3*) immersed in MeCN, see Fig. 7. The concentrations had a ratio of ∼1:2.4 in favor of the 11-N3* sample. The 2D spectra show two sets of diagonal GSB/ESA features at 2095 cm^{-1} (11-N3) and 2027 cm^{-1} (11-N3*). We note that the absence of any cross peak between the two resonances at all waiting times excludes intermolecular coupling as well as non-resonant energy transfer between the functional groups in the MMLs. A closer look at the lineshapes of the two resonances again reveals an inhomogeneous broadening. Fig. 8 shows the corresponding CLSs as a function of waiting time for 11-N3 (open black circles) and 11-N3* (solid black circles) together with exponential fits (red lines) as described above. Both curves start at values around 0.55 and decay to values around 0.3. The obtained time constants are also very similar for both peaks and exhibit values of 4.5 ± 0.2 ps (11-N3) and 4.9 ± 0.2 ps (11-N3*), respectively. A further comparison with the results obtained above for the pure ML 11-N3 samples (open triangles, 4.4 ± 0.4 ps) indicates that the reduction of the surface concentration of the azide probes has no effect on the spectral diffusion. Thus, it can be concluded that Förster-type vibrational energy transfer does not contribute to spectral diffusion in the MMLs.

DISCUSSION

The results presented above demonstrate that 2D ATR IR spectroscopy allows one to resolve ultrafast vibrational dynamics of organic MLs on thin metallic films. The temporal evolution of 2D IR spectra of two organic azides (2-N3 and 11-N3) has been investigated, for which the vibrational probe exhibits varying distances from the surface. The major observable from the 2D ATR IR spectra is the CLS of the GSB/SE signal. The CLS is a measure of correlation between the pump- and probe frequencies and can be used to characterize contributions to spectral line broadening.[28] Large initial CLS values indicate a high degree of correlation between the pumped and the probed frequencies in the 2D spectrum, and hence, a large degree of instantaneous, or initial, inhomogeneity. In this case, the entire absorption band is composed of a

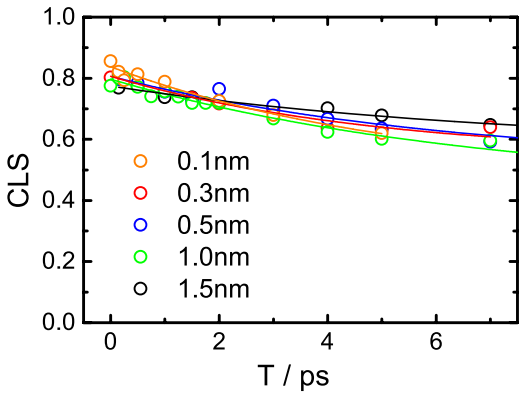

FIG. 6. CLSs of 2-N3 MLs incubated with MeCN in dependence of the sputtered average thickness of the Au layer. Open symbols are experimental data and solid lines represent exponential fits to the data as described in the text.

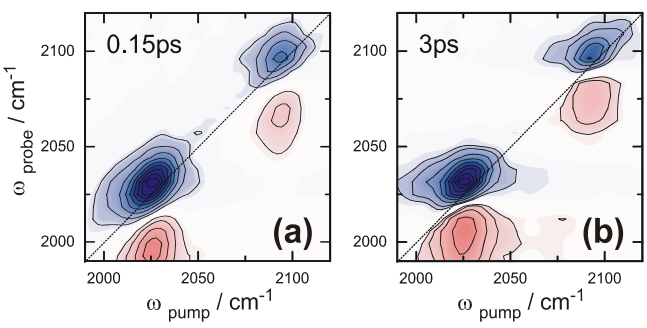

FIG. 7. 2D IR spectra of MMLs formed from 11-N3 and 11-N3* immersed with MeCN at waiting times of (a) 0.15 ps and (b) 3 ps. Signal intensities have been normalized to the GSB/SE signals of 11-N3* in order to facilitate comparison.

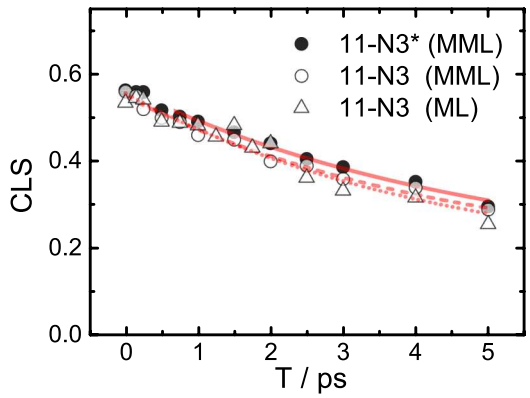

FIG. 8. Spectral diffusion (symbols) together with corresponding exponential fits (red lines) of MMLs 11N3*/11N3 in MeCN (solid and open circles as well as solid and dashed lines, respectively) compared to the pure ML 11-N3 data (open triangles and dotted line, same as in Fig. 5).

distribution of individual bands, each of which belonging to a set of molecules in different environments. However, different mechanisms affect the instantaneous vibrational frequency of a molecule, some of which may be static while others exhibit a temporal evolution. The temporally evolving part of the CLS (Δ_1) reflects processes, which lead to the loss of memory of the initial frequency, i.e., a decrease of the time-dependent inhomogeneity. Contributions can, for instance, originate from structural flexibility of the sample molecule and its environment. Additional features can stem from rotational dynamics, evolutions of the solvation shell, or changes in mutual interactions, e.g., breaking and formation of hydrogen bonds as well as excitation energy transfer between different subsets of oscillators. On the other hand, the offset (Δ_2) reflects contributions that do not evolve on the accessible time window of the 2D IR experiment, i.e., during vibrational relaxation. Such features can be reflected, for instance, by very slowly evolving molecular conformations or molecules in static environments such as the surface morphology.

The main results of the CLS analysis presented here are that (i) the origin of spectral diffusion is the structural flexibility within the ML, and not a Förster-like energy transfer between ML molecules, (ii) the solvation environment affects the dynamics only marginally, but that (iii) the different chain lengths cause significantly different levels of time-dependent inhomogeneities. In the following, we will discuss the origins of the specific differences in the spectral diffusion dynamics.

Environmental influence on spectral diffusion

First, we concentrate on the dynamic feature of the CLS' decays (Δ_1 and τ_{SD}). Different previous works explored the applicability of azide probes as reporters for ultrafast molecular dynamics.[38,54–57] In these studies, spectral diffusion of azide groups covalently attached to different alkyl backbones in bulk solution and different polar and apolar environments generally occurred with rather short time constants in a range of ≈0.5–2 ps.[38,54,55,57] This indicates a generally rapid loss of correlation for the azide vibrational probe. Comparing these values to the ML samples reported here, the spectral diffusion times are slower by at least a factor of 2–3 (Tables I and II). This indicates that either structural dynamics of the sample molecules (e.g., internal rotation of methylene groups in the alkyl chain as well as rotation of the azide group) or environmental influences (e.g., hydrogen-bonding or solvation) are affected by the immobilization process.

The different contributions to spectral diffusion can be disentangled by considering the influence of the solvent. For both ML samples, there is only little variation in the spectral diffusion dynamics with solvent properties. That is, neither a variation of the hydrogen-bonding capability of the solvent (MeCN vs. MeOH) nor its polarity (e.g., MeCN vs. DEE) results in a strong change of the time constants for both the 11-N3 (≈4 ps) and the 2-N3 MLs (≈7 ps, see Fig. 5 and Tables I and II). Therefore, the decelerated spectral diffusion for the ML samples, as compared to bulk solution, must originate mostly from variations in intramolecular dynamics and intermolecular interaction among the sample molecules within the MLs.

Chain-length-dependence

When comparing 11-N3 and 2-N3, we observe significantly different starting values as well as offsets (Δ_2) of the spectral diffusion curves (Fig. 5), indicating different degrees of initial inhomogeneity, which originates from different local conformations of the azide chromophore in the MLs. The initial inhomogeneity is larger for the shorter alkyl chain in 2-N3 as compared to 11-N3. This result might be explained by packing effects of the alkyl chains of different lengths within the ML on the Au surface, which favor, e.g., *trans* over *gauche* conformations within the alkyl-chains.[58] In this context, 11-N3 may be regarded as a good candidate for well-ordered MLs on metal films, as the long alkyl chains of the molecule enable a stronger hydrophobic interaction between the co-adsorbed molecules.[20,59]

With respect to packing of the molecules in the ML samples, it is worth noting that differences exist in the offsets (Δ_2) from the CLS curves of bare and solvated 2-N3 samples while they do not for the 11-N3 samples (Fig. 5). The different values observed for 2-N3 samples indicate that polarity of the solvent is a more determining factor as compared to, e.g., hydrogen-bonding capabilities. This result indicates that the solvent indeed influences the structure of the MLs to a small extend, albeit only for 2-N3. A possible origin might be that the less ordered, less hydrophobic 2-N3 MLs allow for easier penetration of polar solvent molecules in the MLs, while stronger hydrophobic interaction in 11-N3 MLs prevents this effect.

It is illustrative to compare the present results with those of a recent study,[60] which investigated the CO stretching vibrations of a metal-tricarbonyl complex that was covalently attached to alkyl chains immobilized on a silica substrate. In contrast to our observation, the initial distribution of the transition frequencies was essentially independent of chain-length in this case. One difference might be the different nature of the vibrational probe. That is, the metal-carbonyl complexes exhibit fairly bulky organic ligands (phenanthroline), in contrast to the small azide probes employed here. As a result, it may be expected that the alkyl chains exhibit different mutual interactions for the different samples. This is likely to influence

packing of the ML chains on the surface and its different interaction with the solvent molecules. A second difference between the two studies is the preparation of the supporting layers for attachment of the MLs to the surface. While we use metal layers, which are prepared by sputtering, the silica layers used for the metal-carbonyl complexes were of different chemical nature, much thicker (40 nm) and prepared by chemical vapor deposition. As a result, the actual surface morphologies can be significantly different and this will influence sample heterogeneity as reflected by the CLS values.

Heterogeneity of the metal layer

The presented 2D ATR IR experiments show that spectral diffusion occurs largely independent of the average thickness of the Au metal layer (Fig. 6). Both the range of obtained time constants (5.5–7.5 ps) for spectral diffusion as well as the retrieved offsets ($\Delta_2 \approx 0.45$–0.55) can be regarded as similar. Sputtered gold surfaces of very thin average thickness (<1 nm) are expected to result in inhomogeneous surface morphologies.[61,62] In that sense, the very minor dependence of spectral diffusion on the average metal layer thickness indicates that spectral diffusion is not influenced by the metal layers on the time scales that we are able to investigate. That conclusion provides further evidence that the differences observed between 11-N3 and 2-N3 stem from inter- and intramolecular interactions of the sample molecules themselves.

General context of spectral diffusion at interfaces

Multi-dimensional signals from monolayer-forming samples have been reported previously obtained in transmission 2D IR[17,49,60] or with 2D SFG[24,27] spectroscopy. These studies demonstrated the usefulness of multi-dimensional spectroscopy regarding the resolution of intermolecular interactions,[17,24] vibrational dephasing and relaxation, as well as spectral diffusion from samples at interfaces.[16,19,49] For instance, variations in spectral diffusion and vibrational relaxation dynamics have been discussed between octahedral rhenium-carbonyl photocatalysts at silica interfaces and in bulk solution,[16,49] revealing that spectral diffusion at surfaces is slower than in bulk solution. This effect was attributed to interactions of molecules within the monolayer and variations in structural evolution. The observed lengthening of spectral diffusion time scales between bulk solvents and ML samples was determined to be more than one order of magnitude. This general trend of decelerated spectral diffusion for immobilized samples is in clear agreement with a comparatively slow spectral diffusion for azide samples as reported here. The possibly more drastic increase in time constants reported earlier might be reasoned by the specific structures of the investigated samples where the tightly bound carbonyl groups in metal complexes exhibit significant rigidity which can slow down intramolecular contributions to spectral diffusion. This is opposed to the rather flexible sample molecules investigated here, in which the linear alkyl chains as well as the azide functional group can be expected to move with less conformational restriction. This interpretation is supported by the clear observation of ultrafast spectral diffusion (4–6 ps, Tables I and II) in the bare MLs of 2-N3 and 11-N3, for which spectral diffusion is nearly one order of magnitude faster as compared to the previously measured Re-complex.[16,49]

Finally, we have shown that no vibrational energy transfer between ML molecules occurs even at the highest surface concentrations (Figs. 7 and 8). Comparable investigations have been performed recently for water at water-air interfaces[51] or metal-carbonyl MLs on silica.[16,50] In the first case, spectral diffusion is dominated by vibrational energy transfer.[51] Conversely, energy-transfer between different molecules in metal-carbonyl MLs was excluded by means of spectral diffusion measurements for chemically diluted samples, i.e., MLs containing a mixture of molecules, only a fraction of which containing the vibrational chromophore.[50] Chemical dilution experiments are thus very useful, but due to the different chemical properties of the end groups, it is challenging to retain the actual structure of the MLs. This is why the experiments presented here (Figs. 7 and 8) employed the strategy of isotope-dilution of the vibrational probe at the interface which, however, arrived at the same conclusion of absent vibrational energy transfer as in earlier studies.[50]

CONCLUSION

Vibrational dynamics and infrared spectra of organic molecules at metal surfaces are of significant interest. For instance, organic MLs are known to be widely applicable as building blocks for interfacial molecular recognition, nanofabrication and lithography, control of dielectric surface properties, or stabilization of metal nanoparticles.[10,21,63] Using metal surfaces for the immobilization of molecules furthermore allows investigation of vibrational dynamics at purposely charged interfaces as well as redox-induced chemical conversion, since even very thin metal layers (≈1 nm) exhibit conductivity to be usable as electrodes.[61]

Spectroscopic techniques for detailed investigations regarding structural properties and dynamics within MLs are highly desirable but rare. 2D IR spectroscopy has matured over the past decade to a robust and reliable tool in determination of molecular properties, dynamics, chemical interaction and exchange, or energy transfer between different molecules.[28,29] It is thus desirable to directly transfer elaborated multi-dimensional techniques to new experimental configurations which allow investigations of interfacial dynamics. 2D ATR IR spectroscopy is therefore expected to serve as a versatile tool in future to study solid-liquid and solid-gas interfaces as well as ultrafast spectro-electrochemistry.

In the present paper, we have applied 2D ATR IR spectroscopy to resolve the ultrafast dynamics of azide-containing MLs. The azide group is a common vibrational probe in static and time-resolved infrared spectroscopy for the investigation of structural dynamics and environmental interactions.[38,40,54–57] Formation of the monolayers results in a rather slow spectral diffusion for samples with two and 11 methylene groups between the azide group and the surface. Generally, an increase in length of the alkyl chain between the surface of immobilization and the vibrational probe also results in

a smaller time-dependent inhomogeneity. Impacts on spectral diffusion with respect to solvent properties such as solvent polarity and hydrogen-bonding capabilities have been furthermore investigated and reveal that the dominant contribution to spectral diffusion originates from ultrafast intra- and intermolecular dynamics within the monolayers and not from intermolecular interactions with the solvation shell of the azide group. Finally, isotope-dilution experiments for the azide vibrational probe revealed the absence of resonant and non-resonant excitation energy transfer within the monolayer as well as absent coupling between the different functional groups.

Despite its wide application, the azide group exhibits, however, a shortcoming of a rather short vibrational lifetime (≈1 ps) as compared to other vibrational probes such as metal-carbonyls[16,49] or thiocyanates.[64,65] Such probes will extend the observation time window. Independent of that, the azide group is attractive also because of the simple routes it enables to chemically modify the resulting MLs by using straightforward "click"-chemistry.[37,41,49] This will allow for structural and electrostatic investigations of samples with higher complexity such as immobilized proteins[38,66] or polymers,[67,68] and will open up a broad range of future applications of the 2D ATR IR technique such as ultrafast spectro-electrochemistry or multi-dimensional spectroscopy at biological interfaces.

ACKNOWLEDGMENTS

Experimental support from the Center of Microscopy and Image Analysis (University of Zürich) for the preparation of the metal layers is gratefully acknowledged. The authors would like to thank Rolf Pfister (University of Zürich) for the synthesis of the 2-N3 and 11-N3 samples. Discussions with Oliver Zerbe (Organic Chemistry Department, University of Zürich) regarding NMR signals is also gratefully acknowledged. The work has been supported by the Swiss National Foundation (Grant No. CRSII2_136205/1) and by the University Research Priority Program (URPP) for solar light to chemical energy conversion (LightChEC).

[1]P. Rodriguez, Y. Kwon, and M. T. M. Koper, Nat. Chem. **4**, 177 (2012).
[2]J.-M. Andanson and A. Baiker, Chem. Soc. Rev. **39**, 4571 (2010).
[3]F. Zaera, Chem. Soc. Rev. **43**, 7624 (2014).
[4]D. Lis, E. H. G. Backus, J. Hunger, S. H. Parekh, and M. Bonn, Science **344**, 1138 (2014).
[5]M. A. Fox and M. T. Dulay, Chem. Rev. **93**, 341 (1993).
[6]C. Hess, S. Funk, M. Bonn, D. N. Denzler, M. Wolf, and G. Ertl, Appl. Phys. A: Mater. Sci. Process. **71**, 477 (2000).
[7]C. Witham, W. Huang, C.-K. Tsung, J. N. Kuhn, G. A. Somorjai, and F. D. Toste, Nat. Chem. **2**, 36 (2010).
[8]A. Hagfeldt, G. Boschloo, L. Sun, L. Kloo, and H. Pettersson, Chem. Rev. **110**, 6595 (2010).
[9]A. Yella, H.-W. Lee, H. N. Tsao, C. Yi, A. K. Chandiran, M. K. Nazeeruddin, E. W.-G. Diau, C.-Y. Yeh, S. M. Zakeeruddin, and M. Grätzel, Science **334**, 629 (2011).
[10]C. Vericat, M. E. Vela, G. Benitez, P. Carro, and R. C. Salvarezza, Chem. Soc. Rev. **39**, 1805 (2010).
[11]C. Wu, A. B. Khanikaev, R. Adato, N. Arju, A. A. Yanik, H. Altug, and G. Shvets, Nat. Mater. **11**, 69 (2012).
[12]S. A. DiBenedetto, A. Facchetti, M. A. Ratner, and T. J. Marks, Adv. Mater. **21**, 1407 (2009).
[13]D. Samanta and A. Sarkar, Chem. Soc. Rev. **40**, 2567 (2011).
[14]X. Jiang, D. A. Bruzewicz, A. P. Wong, M. Piel, and G. M. Whitesides, Proc. Natl. Acad. Sci. U. S. A. **102**, 975 (2005).
[15]Y.-H. Deng, L.-H. Li, J. He, M. Li, Y. Zhang, X.-M. Wang, F.-Z. Cui, and H. Xia, Mol. Med. Rep. **11**(2), 975 (2014).
[16]D. E. Rosenfeld, Z. Gengeliczki, B. J. Smith, T. D. P. Stack, and M. D. Fayer, Science **334**, 634 (2011).
[17]J. E. Laaser, R. Christianson, T. A. Oudenhoven, Y. Joo, P. Gopalan, J. R. Schmidt, and M. T. Zanni, J. Phys. Chem. C **118**, 5854 (2014).
[18]W. Xiong, J. E. Laaser, P. Paoprasert, R. A. Franking, R. J. Hamers, P. Gopalan, and M. T. Zanni, J. Am. Chem. Soc. **131**, 18040 (2009).
[19]S. Nihonyanagi, A. Eftekhari-Bafrooei, and E. Borguet, J. Chem. Phys. **134**, 084701 (2011).
[20]A. Ulman, Chem. Rev. **96**, 1533 (1996).
[21]J. C. Love, L. A. Estroff, J. K. Kriebel, R. G. Nuzzo, and G. M. Whitesides, Chem. Rev. **105**, 1103 (2005).
[22]A. Eftekhari-Bafrooei and E. Borguet, J. Am. Chem. Soc. **132**, 3756 (2010).
[23]A. Eftekhari-Bafrooei and E. Borguet, J. Am. Chem. Soc. **131**, 12034 (2009).
[24]J. Bredenbeck, A. Ghosh, M. Smits, and M. Bonn, J. Am. Chem. Soc. **130**, 2152 (2008).
[25]J. P. Kraack, D. Lotti, and P. Hamm, J. Phys. Chem. Lett. **18**, 2325 (2014).
[26]C.-S. Hsieh, M. Okuno, J. Hunger, E. H. G. Backus, Y. Nagata, and M. Bonn, Angew. Chem., Int. Ed. Engl. **53**, 8146 (2014).
[27]W. Xiong, J. E. Laaser, R. D. Mehlenbacher, and M. T. Zanni, Proc. Natl. Acad. Sci. U. S. A. **108**, 20902 (2011).
[28]P. Hamm and M. Zanni, *Concepts and Methods of 2D Infrared Spectroscopy* (Cambridge University Press, 2011).
[29]M. Cho, Chem. Rev. **108**, 1331 (2008).
[30]T. Bürgi, Phys. Chem. Chem. Phys. **3**, 2124 (2001).
[31]F. Zaera, Chem. Rev. **112**, 2920 (2012).
[32]J. Helbing and P. Hamm, J. Opt. Soc. Am. B **28**, 171 (2010).
[33]L. P. DeFlores, R. A. Nicodemus, and A. Tokmakoff, Opt. Lett. **32**, 2966 (2007).
[34]S. Nihonyanagi, J. A. Mondal, S. Yamaguchi, and T. Tahara, Annu. Rev. Phys. Chem. **64**, 579 (2013).
[35]P. Hamm, R. A. Kaindl, and J. Stenger, Opt. Lett. **25**, 1798 (2000).
[36]J. P. Collman, N. K. Devaraj, T. P. A. Eberspacher, and C. E. D. Chidsey, Langmuir **22**, 2457 (2006).
[37]J. P. Collman, N. K. Devaraj, and C. E. D. Chidsey, Langmuir **20**, 1051 (2004).
[38]R. Bloem, K. Koziol, S. A. Waldauer, B. Buchli, R. Walser, B. Samatanga, I. Jelesarov, and P. Hamm, J. Phys. Chem. B **116**, 13705 (2012).
[39]M. J. Tucker, Y. S. Kim, and R. M. Hochstrasser, Chem. Phys. Lett. **470**, 80 (2009).
[40]K. Adamczyk, M. Candelaresi, K. Robb, A. Gumiero, M. A. Walsh, A. W. Parker, P. A. Hoskisson, N. P. Tucker, and N. T. Hunt, Meas. Sci. Technol. **23**, 062001 (2012).
[41]S. Zhang and J. T. Koberstein, Langmuir **28**, 486 (2012).
[42]E. Johnson and R. Aroca, J. Phys. Chem. **99**, 9325 (1995).
[43]D. Enders, T. Nagao, A. Pucci, T. Nakayama, and M. Aono, Phys. Chem. Chem. Phys. **13**, 4935 (2011).
[44]T. Lummerstorfer, J. Kattner, and H. Hoffmann, Anal. Bioanal. Chem. **388**, 55 (2007).
[45]P. M. Donaldson and P. Hamm, Angew. Chem. **125**, 662 (2013).
[46]R. Aroca, *Surface-Enhanced Vibrational Spectroscopy* (John Wiley & Sons, Ltd., Chichester, UK, 2006).
[47]M. Osawa, in *Near-F. Opt. Surf. Plasmon Polaritons*, edited by S. Kawata (Springer-Verlag, Berlin, Heidelberg, 2001), pp. 163–187.
[48]K. Kwak, S. Park, I. J. Finkelstein, and M. D. Fayer, J. Chem. Phys. **127**, 124503 (2007).
[49]D. E. Rosenfeld, J. Nishida, C. Yan, S. K. K. Kumar, A. Tamimi, and M. D. Fayer, J. Phys. Chem. C **117**, 1409 (2013).
[50]D. E. Rosenfeld, J. Nishida, C. Yan, Z. Gengeliczki, B. J. Smith, and M. D. Fayer, J. Phys. Chem. C **116**, 23428 (2012).
[51]Z. Zhang, L. Piatkowski, H. J. Bakker, and M. Bonn, Nat. Chem. **3**, 888 (2011).
[52]S. Woutersen and H. J. Bakker, Nature **402**, 507 (1999).
[53]L. Piatkowski, K. B. Eisenthal, and H. J. Bakker, Phys. Chem. Chem. Phys. **11**, 9033 (2009).
[54]S. Dutta, Y.-L. Li, W. Rock, J. C. D. Houtman, A. Kohen, and C. M. Cheatum, J. Phys. Chem. B **116**, 542 (2012).
[55]M. J. Tucker, X. S. Gai, E. E. Fenlon, S. H. Brewer, and R. M. Hochstrasser, Phys. Chem. Chem. Phys. **13**, 2237 (2011).
[56]K. Oh, J. Lee, C. Joo, H. Han, and M. Cho, J. Phys. Chem. B **112**, 10352 (2008).

[57]M. C. Thielges, J. Y. Axup, D. Wong, H. S. Lee, J. K. Chung, P. G. Schultz, and M. D. Fayer, J. Phys. Chem. B **115**, 11294 (2011).
[58]V. V. Naik and S. Vasudevan, J. Phys. Chem. C **113**, 8806 (2009).
[59]A. Kühnle, Curr. Opin. Colloid Interface Sci. **14**, 157 (2009).
[60]J. Nishida, C. Yan, and M. D. Fayer, J. Phys. Chem. C **118**, 523 (2014).
[61]A. I. Stognij, N. N. Novitskii, S. D. Tushina, and S. V. Kalinnikov, Tech. Phys. **48**, 745 (2003).
[62]J. Siegel, O. Lyutakov, V. Rybka, Z. Kolská, and V. Svorčík, Nanoscale Res. Lett. **6**, 96 (2011).
[63]S. Flink, F. C. J. M. Van Veggel, and D. N. Reinhoudt, Adv. Mater. **12**, 1315 (2000).
[64]K.-I. Oh, J.-H. Choi, J.-H. Lee, J.-B. Han, H. Lee, and M. Cho, J. Chem. Phys. **128**, 154504 (2008).
[65]L. J. G. W. van Wilderen, D. Kern-Michler, H. M. Müller-Werkmeister, and J. Bredenbeck, Phys. Chem. Chem. Phys. **16**, 19643 (2014).
[66]I. Radu, M. Schleeger, C. Bolwien, and J. Heberle, Photochem. Photobiol. Sci. **8**, 1517 (2009).
[67]B. Muktha, G. Madras, T. N. G. Row, U. Scherf, and S. Patil, J. Phys. Chem. B **111**, 7994 (2007).
[68]K. T. Oppelt, J. Gasiorowski, D. A. M. Egbe, J. P. Kollender, M. Himmelsbach, A. W. Hassel, N. S. Sariciftci, and G. Knör, J. Am. Chem. Soc. **136**, 12721 (2014).